Appl. Phys. B 53, 296–307 (1991)

Applied Physics B Photophysics and Laser Chemistry

Ultrafast Optical Response in Polydiacetylenes and Polythiophenes

M. Yoshizawa, A. Yasuda, and T. Kobayashi

Department of Physics, Faculty of Science, University of Tokyo, 7-3-1 Hongo, Bunkyo-ku, Tokyo 113, Japan

Received 30 April 1991/Accepted 13 September 1991

Abstract. Ultrafast optical response in the films of poly(3-dodecylthiophene) (P3DT) and blue- and red-phase polydiacetylenes (PDA-4BCMU) has been investigated by femtosecond absorption and picosecond luminescence spectroscopies. Several nonlinear optical processes, i.e., hole burning, Raman gain, inverse Raman scattering, and induced-frequency shift, have been observed. The relaxation processes from photoexcited free excitons to self-trapped excitons (STEs) has been observed. The time constant is estimated as 140 ± 40 fs in the blue-phase PDA-4BCMU and 100 ± 50 fs in P3DT. The generated unthermalized STEs thermalize with the time constant of about 1 ps. The STEs in the blue-phase PDA-4BCMU decay exponentially with lifetime of 1.6 ± 0.1 ps at 290 K and 2.1 ± 0.2 ps at 10 K. The decay curves in the red-phase PDA-4BCMU and P3DT are not single exponential but can be fitted to biexponential functions with time constants of slightly shorter than 1 ps and about 5 ps. These two decay time constants correspond to relaxations to the ground state, respectively, from the free exciton and unthermalized STE and from the thermalized STE.

PACS: 42.62.–k, 71.35.+z, 78.65.Jd

Optical and electrical properties of conjugated polymers have attracted enormous attention because of their large and fast optical nonlinearities and the role as model compounds for quasi-one-dimensional semiconductors. Recent progress in the field of high speed optoelectronics has encouraged the search for new materials with large third-order nonlinear optical susceptibilities [1]. Conjugated polymers are very promising candidates for future practical applications in nonlinear optical devices because of their large varieties of main chains and side groups. Among conjugated polymers, polyacetylene (PA), polydiacetylenes (PDAs), and polythiophenes (PTs) are extensively investigated.

PA possesses the simplest backbone structure of the conjugated ethene type $\text{-}(\text{CH}=\text{CH})_n\text{-}$ main chain. Both *trans* and *cis* forms of PA display large optical nonlinearities [2, 3]. Many theoretical and experimental works have been actively performed on *trans*-PA because of the existence of localized excitations called solitons [4]. The ultrafast relaxation of photoexcited soliton–antisoliton pairs were observed by femtosecond absorption spectroscopy [5, 6]. The soliton pair disappears by intrachain recombination in the picosecond region. The interchain excitation of polarons was observed in oriented PA film [7, 8]. A polaron pair is generated from the electron–hole pair which is photoexcited in different chains. Aftr photoexcitation polarons disappear by the interchain relaxation mechanism in nanoseconds to microseconds depending on the intensity of the interchain interaction.

PDAs possess the diacetylene-type configuration $\text{-}(\text{CR}_1\text{-C}\equiv\text{C-CR}_2)_n\text{-}$ and have several remarkable characteristics. The properties of PDAs can be modified considerably by changing the side groups R_1 and R_2. The polymerization of a large number of diacetylenes with various side groups has been reported. PDAs can be obtained in the form of highly ordered single crystals, Langumuir-Blodgett films, vacuum deposited films, and solvent-cast films [9]. Another characteristic of PDAs is dramatic color changes. Several PDA films and crystals have two phases called blue-phase and red-phase according to the color. The phase transition can be induced by photoirradiation, pressure and heat [10, 11]. Red-phase PDAs have weak fluorescence with the quantum yield of $< 10^{-(3-4)}$ [12], while blue-phase PDAs have no fluorescence. Until several years ago it was supposed that the color changes were due to two possible chemical structures of the main chain of PDAs, acetylenic $\text{-}(\text{CR-C}\equiv\text{C-CR})_n\text{-}$ and butatrienic $\text{-}(\text{CR}=\text{C}=\text{C}=\text{CR})_n\text{-}$. However, recent X-ray diffraction study has shown that both blue- and red-phase PDAs have the acetylenic main

chain [13]. The phase transition of PDAs with alkyl-urethane side-groups is accompanied not only by the change in the backbone structure but also by the conformational changes of alkyl chains [10]. However, the electronic structures of these phases have not been clearly established.

Recent interest in PDAs has been focused on their large nonlinear optical susceptibility and ultrafast optical response. Various third-order nonlinear processes such as the degenerate four-wave mixing [14, 15], third-harmonic generation [16, 17], coherent-Raman scattering [18], inverse Raman spectroscopy [19], optical Kerr effect [20, 21], and absorption saturation [22, 23] have been extensively studied. PDAs have ultrashort phase and energy relaxation times, T_2 [14, 18] and T_1 [24–27], respectively. The time constants of 150 fs and 1.5 ps were observed in the decay kinetics of blue-phase PDA-3BCMU [25], and assigned respectively to the formation and relaxation processes of self-trapped excitons (STEs).

PTs have a ring structure in their repeating unit. The backbone geometry resembles that of *cis*-PA and the simple *cis*-like structure is stabilized by the sulfur. The ultrafast dynamics has been also extensively investigated in PTs [28–31]. Ultrafast relaxation processes and several nonlinear optical effects, i.e., hole burning, Raman gain, and optical Kerr effect, were observed in poly(3-methylthiophene) (P3MT) films [28]. The obtained decay time was 800 ± 100 fs at 10 K and the relaxation process was explained in terms of STEs. It is well established by stationary spectroscopies and photoinduced electron-spin resonance experiments that polarons and bipolarons are formed in PTs after photoexcitation or electrochemical doping [32–34]. The bipolaron formation is due to the nondegenerate ground state in PTs, which leads to the confinement of soliton-antisoliton pairs because of inequivalence of energy between phenyl and quinoid forms. The photoluminescence of PTs has been reported to be due to either free charge carriers or excitons [35]. It has been suggested that generation of photoluminescent excitons is independent of the formation of polarons or bipolarons.

In this study the ultrafast optical response in blue- and red-phase PDA-4BCMU (4-butoxycarbonylmethylurethane) and P3DT [poly(3-dodecylthiophene)] films were investigated by femtosecond absorption and picosecond luminescence spectroscopies. The third-order nonlinear optical susceptibilities of various processes were determined. The mechanisms of the ultrafast relaxation in conjugated polymers are discussed in terms of STEs.

1 Experimental

The femtosecond absorption spectroscopy system consists of four parts, a colliding-pulse mode-locked (CPM) ring dye laser, a four-stage dye amplifier pumped by the second harmonic pulses of a 10 Hz Q-switched Nd : YAG laser, a grating pair pulse compressor, and an optical system of pump-probe absorption spectroscopy [25]. The wavelength of peak intensity of the amplified pulses changed between 625 nm (1.98 eV) and 630 nm (1.97 eV) by the dye concentrations of the CPM laser and the amplifier. The duration and the energy are 80 fs and about 200 μJ, respectively. The polarization and intensity of the pump pulse were controlled by a half-wave plate and a circular linear-wedge neutral-density filter, respectively. The second harmonic of the amplified femtosecond pulse generated by a 1 mm thick KDP crystal was also used as the pump pulse. The probe white continuum generated by self-phase modulation was detected with a polychromator/multichannel detection system and analyzed by a microcomputer. The time resolution of the system was about 100 fs.

A mode-locked dye laser synchronously pumped by the second harmonic pulses of a cw mode-locked Nd : YAG laser (Spectra Physics, series 3000) was used as a pump source of the picosecond luminescence spectroscopy. The luminescence was detected by a synchroscan streak camera (Hamamatsu, OOS-3085). The resolution time of the whole system was about 30 ps. Measurement of the stationary luminescence spectra was made using a cw argon ion laser (488.3 nm, 2.54 eV), a monochromator (25 cm focal length, a 1200 grooves/mm grating), and a photomultiplier tube (Hamamatsu, R666S). The spectral response of the detection equipment was corrected.

PDA-4BCMU (4-butoxycarbonalmethylurethane) has the side groups of

$$R_1=R_2=-(CH_2)_4OCONHCH_2COO(CH_2)_3CH_3.$$

Oriented films of PDA-4BCMU were prepared from the diacetylene monomers by the following procedure [36]: a vacuum deposition of a thin primary monomer layer on a glass substrate, a photo-polymerization, a mechanical rubbing process, second vacuum deposition of a thicker monomer layer, and final photo-polymerization. The thicknesses of the films wer about 60 nm. The obtained oriented films were blue-phase PDA. Red-phase oriented films were prepared by the thermal annealing of the blue-phase oriented films.

PDA-4BCMU is soluble in several solvents such as chloroform and carbon tetrachloride. This films of PDA-4BCMU were prepared also by casting condensed solution in chloroform on a glass substrate. The cast films of PDA-4BCMU were in the red-phase. The thicknesses of the films were varied between 0.1 and 1.0 μm depending on the purpose of experiment.

P3DT [poly(3-dodecylthiophene)] has the side group of $R=-(CH_2)_{11}CH_3$. Thin films of P3DT were synthesized electrochemically on an In–Sn oxide (ITO) conducting glass substrate. The as-grown films wer undoped electrochemically. The obtained neutral films were peeled off from the ITO glass and stretched uniaxially up to twice the original length [35]. The thicknesses of the P3DT films used in this study were 0.1–2.0 μm.

2 Absorption and Luminescence Spectra of PDA-4BCMU

Figure 1a shows absorption spectra of a blue-phase oriented PDA-4BCMU film at room temperature. The probe

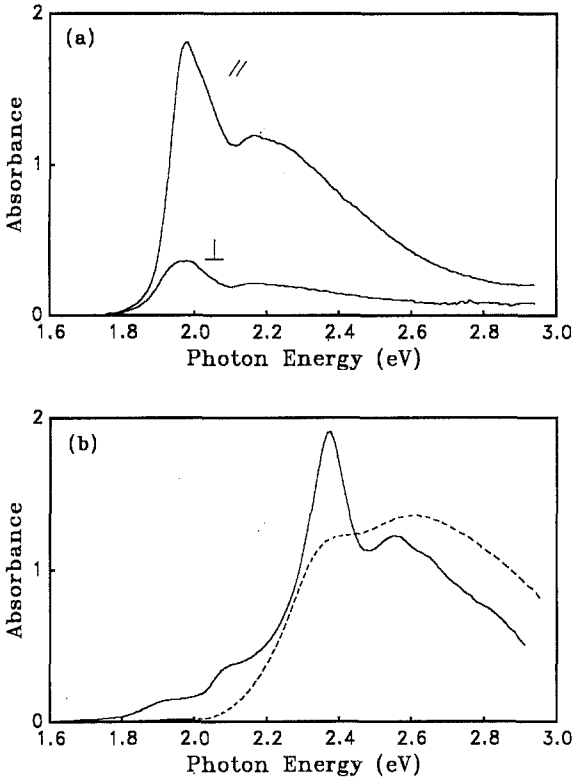

Fig. 1a, b. Absorption spectral of **a** a blue-phase oriented PDA-4BCMU film and **b** a red-phase oriented PDA-4BCMU (solid curve) and a PDA-4BCMU cast film (dashed curve) at room temperature. The probe light is polarized parallel (||) and perpendicular (⊥) to the blue-phase oriented PDA-4BCMU chain

light is polarized parallel (//) and perpendicular (⊥) to the orientation direction of the main chain. The dichroic ratio is about 5. The oriented film of blue-phase PDA-4BCMU has an absorption peak of the lowest singlet (^1B_u) excitons at 1.97 eV. Another absorption peak due to a phonon sideband appears at 2.17 eV.

The absorption spectra of oriented and cast film of red-phase PDA-4BCMU are shown in Fig. 1b. The probe light is polarized parallel to the oriented red-phase polymer chain. The red-phase oriented film prepared by the vacuum deposition has absorption peaks of the exciton and the phonon sidebands at 2.35 eV and 2.55 eV, respectively. The low energy tail of the cast film sample and two shoulders of the oriented film are due to the absorption of residual blue-phase polymers. The exciton peak in the cast film of red-phase PDA-4BCMU is not clear. The absorption of the cast film has a shoulder at 2.35 eV and a peak at 2.6 eV. The broad absorption of the cast film is probably due to inhomogeneous disorder in the polymer chain.

The luminescence spectra of the PDA-4BCMU films pumped by the 2.54 eV light are shown in Fig. 2. The luminescence of the red-phase oriented film has a peak at 2.2 eV. The Stokes shift is about 0.15 eV. The luminescence spectrum of the cast film has two peaks at 2.24 eV and 2.04 eV. The luminescence intensity in the cast film is about 4 times stronger than that in the oriented film and the 2.04 eV peak in the cast film is larger than the 2.24 eV peak. The electron–phonon coupling in the cast film is

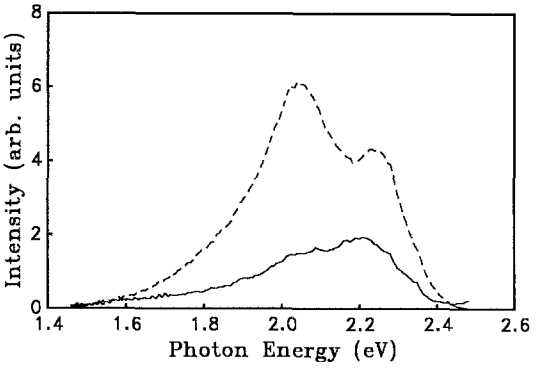

Fig. 2. Luminescence spectra of a red-phase oriented PDA-4BCMU film (solid curves) and a red-phase PDA-4BCMU cast film (dashed curve) at room temperature

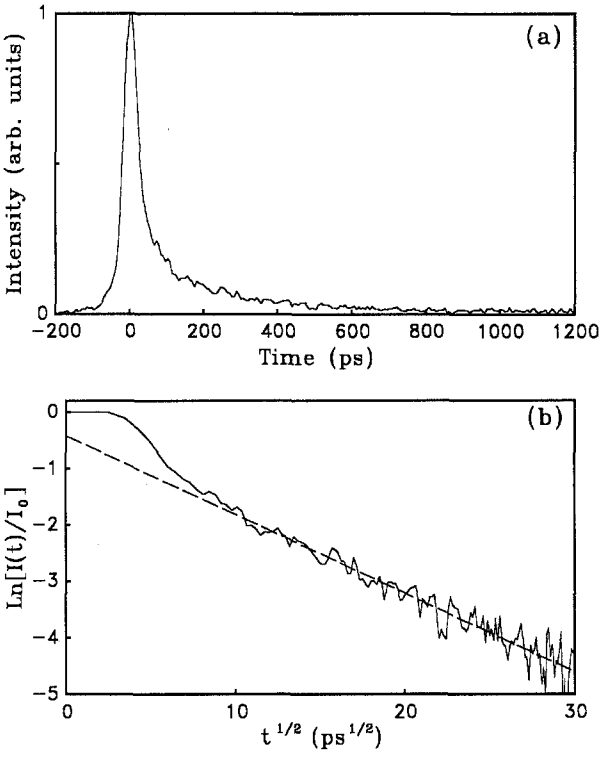

Fig. 3a;b. Time dependence of luminescence at 1.65 eV in a red-phase PDA-4BCMU cast film at 10 K. **a** Linear plot of intensity I vs time t and **b** $\log(I)$ vs $t^{1/2}$. The dashed line indicates the function of $\exp[-(t/\tau)^{1/2}]$ with $\tau = 51$ ps

considered to be stronger than that in the oriented film because of the disorder of the polymers.

Figure 3 shows the time dependence of the luminescence intensity in the red-phase PDA-4BCMU cast film at 10 K pumped by the 2.14 eV picosecond pulse. The decay kinetics of the luminescence has fast and slow components. The lifetime of the fast component is shorter than the resolution time, 30 ps. The decay curve of the slow component can be represented by $\exp[-(t/\tau)^{1/2}]$ as shown in Fig. 3b. The time constant τ is obtained as 51 ± 5 ps at 10 K and 48 ± 5 ps at 290 K. The decay curve of the slow component can be explained by a trapping model that the photoexcited species decays at a trap after random walk in a one-dimensional chain. The initial

decay kinetics ($t \sim \tau$) of the trapping model can be simulated by $\exp[-(t/\tau)^{1/2}]$ [37]. The decay curve of the luminescence in nanoseconds to microseconds was represented by a form of $\exp(-at^{1/3})$ [22, 38]. It is consistent with the decay kinetics of the trapping model for much longer delay time ($t \gg \tau$).

The Stokes shift of the luminescence with long life is larger than the fast component. The peak of the slow component is at 1.9 eV, while the peak of the fast component is higher than 2 eV. The radiative intensity of the slow component normalized to the fast component is about 5 times higher in the cast film than that in the oriented red-phase film. Therefore, the slow component is due to traps in the polymer chain, because the cast film has large disorder. The traps are probably the defects of the conjugation in the main chain. The fast component is considered to be due to photoexcited excitons.

3 Results of Femtosecond Absorption Spectroscopy

3.1 Blue-Phase PDA-4BCMU

Figure 4 shows the stationary and transient photoinduced absorption spectra of the blue-phase oriented PDA-4BCMU film at the delay times when the pump and probe pulses overlap in time in the sample. The polarizations of the pump and probe pulses are parallel to the polymer chain. The peak photon energy of the pump pulses was 1.98 eV when the experiment was done at 290 K and 1.97 eV at 10 K as shown in Fig. 4. The pump photon density was about 2.0×10^{15} photons/cm^2 at both temperatures.

The absorbance changes at −0.2 and −0.1 ps have a bleaching peak at the pump photon energy. The bleaching at 290 K becomes broader with time from −0.1 ps to 0.2 ps and the peak shifts to 1.96 eV. At 10 K the bleaching peak at 1.97 eV disappears very rapidly and another bleaching peak appears at 1.91 eV where the excitons have the absorption peak. The 1.97 eV peak is observed when the pump and probe pulses overlap in time at the sample. It is considered to be due to coherent interaction between the pump and probe pulses. The 1.91 eV peak is due to the saturation of the excitonic absorption.

The absorbance changes below the pump photon energy have two minima at 1.80 and 1.72 eV at 290 K and 1.79 and 1.71 eV at 10 K. These minima were also observed in PDA-3BCMU film and explained in terms of Raman gain [25]. The corresponding Raman shifts are 1470 and 2110 cm^{-1}. They are assigned to the stretching vibrations of the C=C and C≡C bonds, respectively.

Absorbance changes due to the same phonon modes are observed also at the photon energies above the pump. At the delay time of −0.1 ps two small maxima at 2.14 and 2.23 eV are clearly observed in the absorbance change at 10 K. They are due to the inverse Raman scattering. The inverse Raman scattering was observed and minutely studied in PDA-*p*TS [19]. At positive delay times a bleaching peak appears at 2.10 eV. The energy difference from the 1.91 eV bleaching peak is 0.19 eV. The bleaching peak is due to the exciton phonon sideband and the corresponding phonon mode is the C=C strech-ing vibration.

Two small maxima at 2.18 and 2.25 eV are observed also at 290 K. The signals are very small compared with the Raman gain signal and the peak photon energies are different from the peak expected from the inverse Raman scattering signal. It is explained by the overlap of the maxima due to inverse Raman scattering and the minima due to the phonon sidebands, because the absorption peak of the excitons at 290 K is close to the pump photon energy.

The imaginary part of the third-order susceptibilities measured by the pump-probe method can be calculated by using equation

$$\mathrm{Im}[\chi^{(3)}_{1111}(-\omega_2;\omega_2,\omega_1,-\omega_1)] = n(\omega_1)n(\omega_2)ck_2/96\pi^2, \quad (1)$$

where $n(\omega_1)$ and $n(\omega_2)$ are the real refractive indices at the frequencies of ω_1 and ω_2, respectively, and c is the

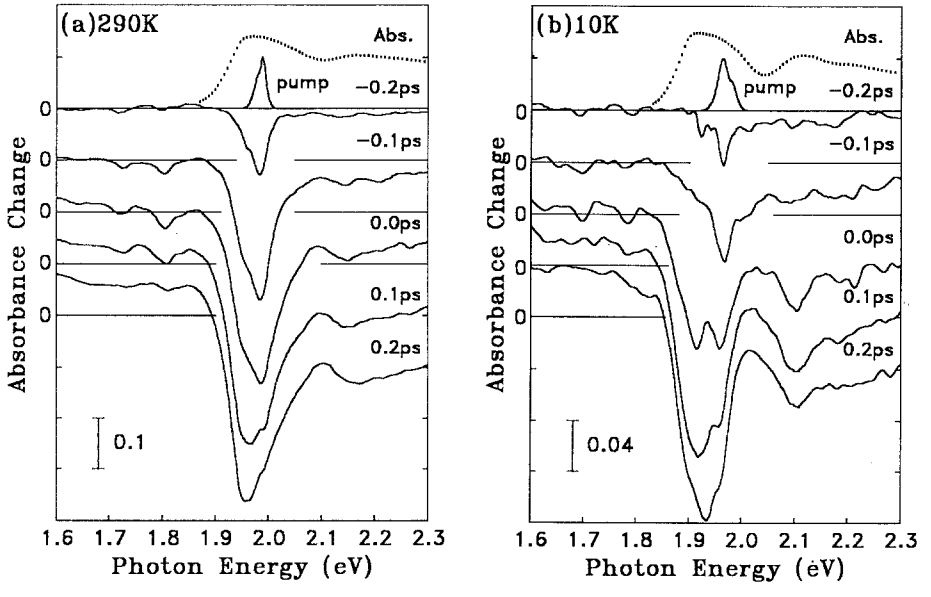

Fig. 4a, b. Transient absorption spectra of a blue-phase oriented PDA-4BCMU film at **a** 290 K and **b** 10 K. The pump and probe pulses are polarized parallel to the polymer chain. The absorption (dotted curves) and pump spectra are shown together. The excitation photon densities are 2.0×10^{15} photons/cm^2

velocity of light in vacuum. The nonlinear extinction coefficient κ_2 can be obtained as

$$\kappa_2 = \Delta\alpha c/2\omega I, \quad (2)$$

where $\Delta\alpha$ is the change of the absorption coefficient and I is the pump intensity.

The third-order susceptibilities in the blue-phase PDA-4BCMU film are calculated using pump photon density of 4.9×10^{14} photons/cm^2 much lower than the saturation photon density of 3×10^{15} photons/cm^2 to avoid a saturation effect of the absorbance change due to the higher-order nonlinearity. The decrease in the pump intensity is taken into account using the absorption coefficient of $\alpha = 2 \times 10^5$ cm^{-1}. $\mathrm{Im}[\chi^{(3)}_{1111}(-\omega_1;\omega_1,\omega_1,-\omega_1)]$ in the blue-phase oriented PDA-4BCMU film at 290 K is obtained as -3.2×10^{-9} esu for $\hbar\omega_1 = 1.98$ eV. The $\mathrm{Im}[\chi^{(3)}_{1111}(-\omega_2;\omega_2,\omega_1,-\omega_1)]$ corresponding to the Raman gain is -4.8×10^{-10} esu for $\hbar\omega_1 = 1.98$ eV and $\hbar\omega_2 = 1.80$ eV. The real part of the refractive indiced are calculated from the absorption spectrum as $n(\omega_1) = 1.9$ and $n(\omega_2) = 1.5$.

The absorbance changes induced by the pump pulse polarized perpendicular to the polymer chain have similar structures to the spectra induced by the parallel pump pulse. The bleaching due to the hole burning and the two minima due to Raman gain areclearly observed. The third-order susceptibilities are obtained as $\mathrm{Im}[\chi^{(3)}_{1111}(-\omega_1;\omega_1,\omega_1,-\omega_1)] = -2.4 \times 10^{-10}$ esu at the pump photon energy $\hbar\omega_1 = 1.98$ eV and $\mathrm{Im}[\chi^{(3)}_{1122}(-\omega_2;\omega_2,\omega_1,-\omega_1)] = -4.0 \times 10^{-11}$ esu for the Raman gain.

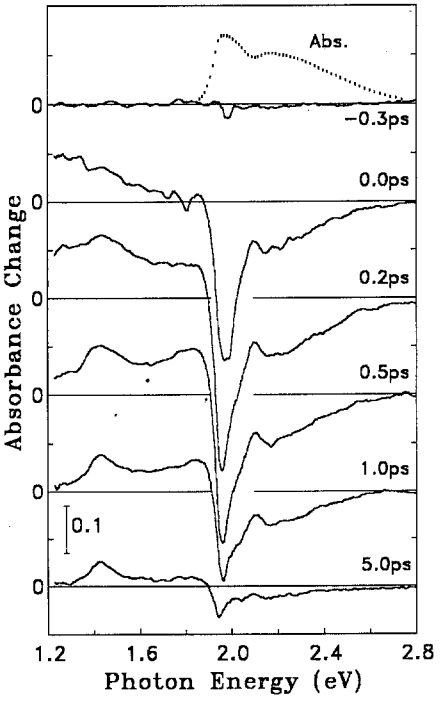

Fig. 5. Transient absorption spectra of a blue-phase oriented PDA-4BCMU film at 290 K induced by the 1.98 eV pump pulse. The excitation photon density is 2.0×10^{15} photons/cm^2. The dotted curve is the absorption spectrum

Figure 5 shows the transient absorption spectra of the oriented PDA-4BCMU film in the blue phase at 290 K up to 5 ps in the spectral range of 1.2–2.8 eV. At 0.0 ps bleaching above 1.9 eV and absorption below 1.6 eV are observed in addition to the above-mentioned nonlinear optical responses. The bleaching is due to the absorption saturation of the ^1B_u excitons. The photoinduced absorption at 0.0 ps has a peak at the photon energy lower than 1.4 eV. Then the absorption shifts to higher energy with time from 0.0 ps to 0.5 ps. The absorption at 0.5 ps has a peak at 1.8 eV. Similar spectral change was also observed in PDA-3BCMU and poly(3-methylthiophene) and was explained in terms of self-trapped excitons (STEs) [22, 25]. The photoinduced absorption is assigned to the transitions from the lowest singlet (^1B_u) excitons to the conduction band and/or other higher excited states. Since the photoexcited free excitons relax to the bottom of the adiabatic potential surfaces of the STEs (relaxed STEs), the transient absorption shifts to higher energy.

The absorbance change at 5.0 ps has an absorption peak at 1.4 eV. This absorbance change remains for much longer than 100 ps. The absorption at 1.4 eV is assigned to triplet excitons [39, 40]. The pump intensity dependence of the singlet excitons shows a linear response [25, 41], while the long-lived component increases superlinearly with the pump intensity. The pump intensity dependence of the triplet excitons was studied in PDA-MADF [41]. The result shows that the population of the triplet excitons is proportional to the square of the singlet exciton population even at higher-pump intensities where the singlet excitons exhibits saturation. The formation mechanism of the triplet excitons generated by the 1.97 eV pump pulse was concluded to be not due to the two-photon absorption but due to the collision of the singlet excitons [41].

Figure 6 shows the time dependences of the absorbance change at several probe photon energies. The absorbance change at 1.23 eV appears just after excitation and disappears very rapidly with the time constant of 210 ± 30 fs. The absorbance change at 1.88 eV is assigned to the relaxed STEs, so it appears slowly. The formation and decay time constants of the relaxed STEs are determined as 140 ± 40 fs and 1.6 ± 0.1 ps, respectively. The decay time constant at 1.23 eV is slightly longer than the rise time at 1.88 eV, because the absorption at 1.23 eV is mainly due to the free excitons but the STEs has also absorption at 1.23 eV during the relaxation process. The time dependence at 1.91 eV is complicated. The absorbance change at 1.91 eV is negative at 0.0 ps because of the absorption saturation of excitons. Then the absorption of the relaxed STEs appears and the absorbance change becomes positive. Finally the STEs disappear and the absorbance change becomes negative again because of the remaining triplet excitons.

The decay curves of the absorbance changes in the blue-phase PDA-4BCMU can be fitted to single-exponential functions and long-lived component, $\Delta A \exp(-t/\tau) + \Delta A_L$. The obtained time constants are summarized in Table 1. The lifetime depends on the probe photon energy. The time constant around 1.9 eV which corresponds to the lifetime of the relaxed STE is

Table 1. Decay time constants of absorbance changes in a blue-phase oriented PDA-4BCMU film

Probe photon energy [eV]	Decay time [ps]	
	290 K	10 K
2.21	1.1 ± 0.1	1.2 ± 0.1
1.97	1.1 ± 0.1	1.5 ± 0.1
1.91	1.6 ± 0.3	2.1 ± 0.3
1.88	1.6 ± 0.1	2.0 ± 0.3
1.77	1.2 ± 0.1	2.1 ± 0.2
1.41	0.5 ± 0.1	1.1 ± 0.2
1.23	0.2 ± 0.1	0.3 ± 0.1

about 1.6 ps. The decay kinetics below 1.7 eV is mainly the blue shift of the photoinduced absorption caused by the formation of the relaxed STEs, so the time constant is shorter than 1 ps. The bleaching above 1.95 eV is due to both the free excitons and the relaxed STEs. The relaxation from the free excitons to the ground state is expected to be faster than that from the relaxed STEs. However, the decay kinetics of the free excitons and the relaxed STEs could not be distinguished in the blue-phase PDA-4BCMU. The observed lifetime of the bleaching is about 1 ps.

The transient absorbance changes of the oriented PDA-4BCMU film at 10 K are similar to the changes at 290 K. The bleaching due to the absorption saturation of the excitons, the broad absorption below the absorption edge, and the blue-shift of the photoinduced absorption are observed. The formation time of the relaxed STEs is estimated as 120 ± 30 fs and is almost same with the time constant at 290 K. It is consistent with the barrierless potential of the STE in one-dimensional systems [42]. The lifetime of the relaxed STE is obtained as 2.1 ± 0.2 ps. It is longer than the lifetime at 290 K, but the difference is small. This suggests that the main relaxation process is a tunneling in configuration space from the STEs to the ground state.

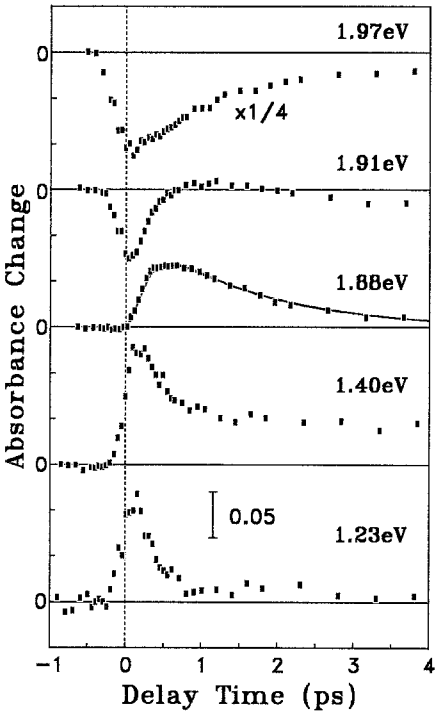

Fig. 6. Time dependence of absorbance changes in a blue-phase oriented PDA-4BCMU film at 290 K. A solid curve at 1.88 eV is the calculated transient absorbance change with the formation and decay times of 140 fs and 1.6 ps, respectively. The resolution time at 1.88 eV is obtained by a cross-correlation method as 150 fs

3.2 Red-Phase PDA-4BCMU

Figure 7 shows the transient absorption spectra of the red-phase PDA-4BCMU cast film at 290 K excited by the 1.97 eV pump pulse. The observed absorbance change is positive at the whole photon energies shown in the figure. Since the absorption edge of the cast film is 2.0 eV, the 1.97 eV pump pulse cannot directly excite the exciton. The pump intensity dependence of the absorbance change is represented by I^a with $a = 1.9 \pm 0.1$. The observed transient absorption is induced by the two-photon absorption of the 1.97 eV pump pulse.

The two minima due to the Raman gain are observed also in the red-phase cast film at 1.78 eV and 1.71 eV. The corresponding Raman shifts are 1530 and 2130 cm^{-1} and assigned to the stretching vibrations of the C=C and C≡C bonds in red-phase PDA, respectively. The corresponding third-order susceptibility is obtained as $\mathrm{Im}[\chi^{(3)}_{1111}(-\omega_2;\omega_2,\omega_1,-\omega_1)] = -1.4\times10^{-13}$ esu for $\hbar\omega_1 =$ 1.97 eV and $\hbar\omega_2 = 1.78$ eV.

The absorbance change around 1.97 eV in the cast film has an asymmetric oscillatory structure. The absorbance change has a maximum at 1.96 eV and a minimum at 1.99 eV. Similar asymmetric structure has been observed also in a blue-phase PDA-3BCMU film and was tentatively explained by the optical Stark shift of excitons to lower energy [25]. The asymmetric structure due to optical Stark effect was also reported in semiconductors [43]. However, the exciton energy of the red-phase PDA is 2.35 eV and higher than the pump photon energy. When

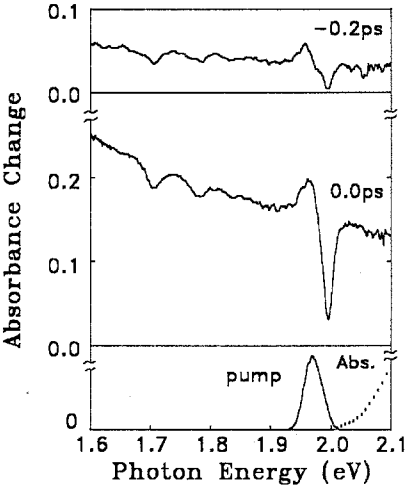

Fig. 7. Transient absorption spectra of a red-phae PDA-4BCMU cast film at 290 K induced by the 1.97 eV pump pulse. The spectrum of pump pulse is shown together. The excitation photon density is 4.0×10^{16} photons/cm^2. The dotted curve is the absorption spectrum

the pump pulse excites the low energy tail of the inhomogeneous broadened exciton peak, the transmittance change has an asymmetric oscillatory structure due to the perturbed free induction decay [44]. The oscillation frequency due to the perturbed free induction decay depends linearly on the delay time, but the observed oscillation does not change the frequency.

The observed asymmetric structure is similar to the differential spectra of the 1.97 eV pump pulse or the probe white continuum pulse generated from the 1.97 eV pulse by the self-phase modulation. The amplitude of the oscillation is proportional to the pump intensity. The structure around 1.97 eV can be explained in terms of induced-frequency shift of probe light [45]. The induced frequency shift can be clarified changing the spectra of the probe pulse. The change of the probe pulse due to the induced frequency shift was clearly found in GaAs microcrystallites [46].

The wavelength shift of the probe light is porportional to the time derivative of the refractive index as

$$\Delta\lambda = \frac{\lambda L}{c}\frac{dn}{dt}, \tag{3}$$

where L is a sample thickness. When the probe light with a peak at 1.97 eV shifts to higher energy, the transmitted probe light above 1.97 eV increases and the light below 1.97 eV decreases. Therefore, the absorbance decreases above 1.97 eV and increases below 1.97 eV. The maximum induced-wavelength shift observed by the pump pulse with the duration of τ_0 is given by

$$\Delta\lambda_{\max} = 2n_2\lambda IL/c\tau_0, \tag{4}$$

where n_2 is the nonlinear refractive index. The shift of the probe pulse is estimated from the oscillation at 0.0 ps as $\Delta\lambda = -0.78$ nm. The n_2 and the third-order susceptibility $\mathrm{Re}[\chi^{(3)}_{1111}]$ are obtained as -2.7×10^{-13} $\mathrm{cm_2/W}$ and -1.9×10^{-12} esu, respectively.

The transient spectra and time dependence of the absorbance change are shown in Figs. 8 and 9, respectively, observed for the red-phase PDA-4BCMU cast film at 290 K excited by the second harmonic (3.94 eV) of the femtosecond pulse. The pulse duration of the 3.94 eV pump pulse was about 200 fs and was longer than the 1.97 eV pulse because of the dispersion in the KDP crystal. The bleaching peaks at 2.36 and 2.60 eV are due to the lowest singlet excitons and the phonon sidebands. The broad absorption below 2.2 eV is expected to be due to the STEs. The spectral shift due to the relaxation from the free excitons to the relaxed STEs is not as clear as in the blue-phase PDA-4BCMU, but the absorption around 2.1 eV appears slightly slower than both the absorption below 2.0 eV and the bleaching. The formation time of the relaxed STE was obtained as 120 ± 60 fs.

The transient absorbance change in the red-phase PDA has also the long-lived component due to the triplet excitons. The lifetime is much longer than 100 ps. The short-lived component in the blue-phase PDA-4BCMU can be fitted to single-exponential functions, but as shown in Fig. 9b the decay in the red-phase PDA-4BCMU becomes slower after the initial fast decay. The decay kinetics at 2.34 eV can be fitted to a biexponential func-

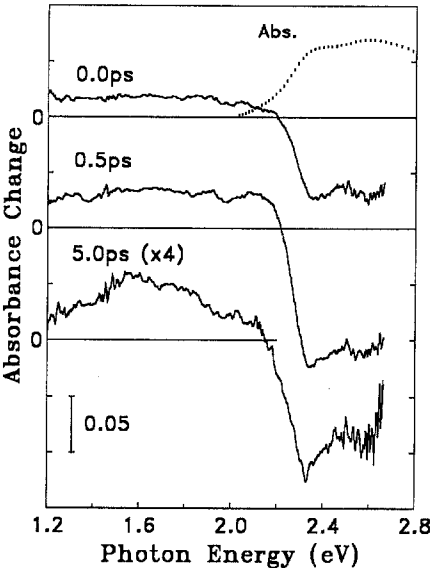

Fig. 8. Transient absorption spectra of a red-phase PDA-4BCMU cast film at 290 K induced by the 3.94 eV pump pulse. The excitation photon density is 1×10^{15} photons/cm^2. The dotted curve is the absorption spectrum

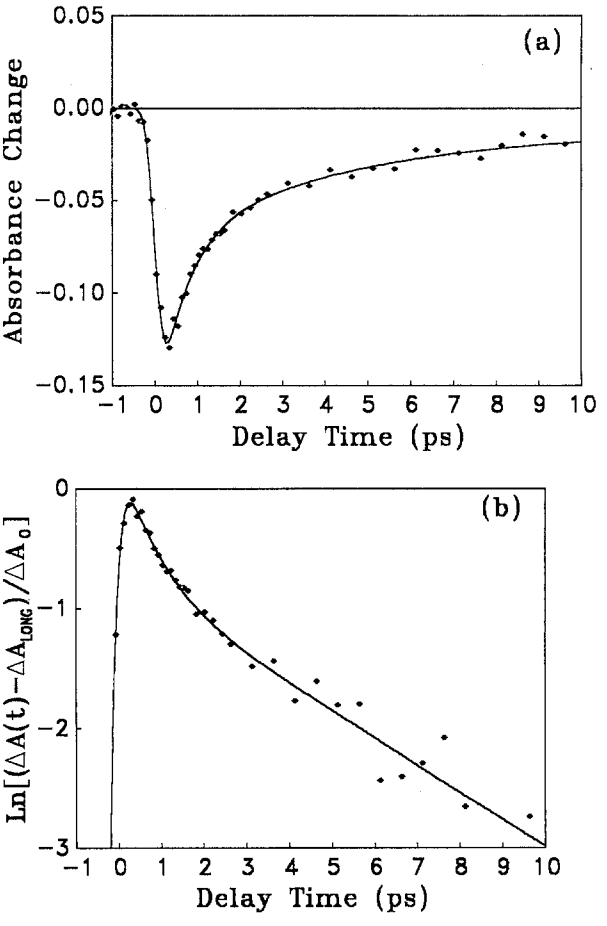

Fig. 9a, b. Time dependence of absorbance change at 2.34 eV in a red-phase PDA-4BCMU cast film at 290 K induced by the 3.94 eV pulse. **a** A linear plot and **b** a semilogarithmic plot. The long-lived component is subtracted from the observed data in the plot **b**. The excitation photon density is 1×10^{15} photons/cm^2. Solid curves are the biexponential function with the decay time constants of 660 fs and 4.4 ps. The resolution time is estimated as 300 fs

Table 2. Decay time constants of absorbance changes in a red-phase cast PDA-4BCMU film at 290 K excited by the 3.94 eV pump pulse

Probe photon energy [eV]	Time constants [ps]	
	τ_1	τ_2
2.58	0.4 ± 0.1	3.5 ± 0.6
2.34	0.7 ± 0.1	4.4 ± 0.5
2.00[a]	1.3 ± 0.3	–
1.77	0.8 ± 0.1	10.0 ± 0.6
1.70	0.9 ± 0.2	8.2 ± 1.4
1.55	1.3 ± 0.3	10.4 ± 2.2

[a] The decay curve at 2.00 eV can be fit to a single-exponential function. The second time constant τ_2 could not be estimated

tion and the long-lived component with the form of $\Delta A_1 \exp(-t/\tau_1) + \Delta A_2 \exp(-t/\tau_2) + \Delta A_L$. The time constants τ_1 and τ_2 are 660 ± 70 fs and 4.4 ± 0.4 ps. The decay curves at each prove photon energies can be fitted to biexponential functions with different sets of the time constants summarized in Table 2. The time constant τ_1 is shorter than 1 ps and corresponds to the relaxation of the free and unrelaxed self-trapped excitons. The time constant τ_2 corresponds to the relaxation of the relaxed STEs and it is longer than that in the blue-phase PDA. The second time constant τ_2 at 2.00 eV could not be determined. The time constant at 2.00 eV is obtained using a single-exponential function.

The decay curves of the absorbance change can be represented by also a power law decay and long-lived component, $\Delta A_1 t^{-\alpha} + \Delta A_L$. The power α is obtained as 0.56 ± 0.03 at 2.34 eV, 0.43 ± 0.07 at 1.77 eV, and 0.34 ± 0.07 at 1.55 eV. The power low decay can be explained using recombination model. However, the dependence of α on the probe wavelength is difficult to the explained by the simple recombination model.

The photoinduced absorption spectra are changed with time from 0.5 ps to 5.0 ps. The absorption below 2.2 eV is almost flat at 0.5 ps. Then absorbance changes around 2.1 eV and 1.2 eV decrease faster than the changes around 1.6 eV. The absorption at 5.0 ps has a peak at 1.55 eV. The time constant of the spectral change is determined from the time dependence of the ratio between the short-lived components at 2.07 eV and 1.61 eV as 1.1 ± 0.1 ps. The bleaching spectra above 2.2 eV are also changed with time. The time constant is estimated from the absorbance changes at 2.34 eV and 2.58 eV as 1.1 ± 0.1 ps. The detailed relaxation kinetics are discussed in Sect. 4.

The photoinduced bleaching and broad absorption are observed also in the oriented red-phase PDA-4BCMU film prepared by the vacuum deposition. The decay curves of the absorbance changes can be fitted to biexponential functions and long-lived component in the same way as the red-phase cast film as shown later in Fig. 12. The time constants of the decay kinetics at 1.77 eV are obtained as 840 ± 60 fs and $10.9 \pm 1,8$ ps at 290 K. The time constants are almost same with those in the red-phase cast film. The absorption and luminescence spectra of the red-phase PDAs are dependent on the preparation methods and the sample quality as shown in Figs. 1 and 2, but the ultrafast decay kinetics is insensitive to the sample preparation method. This suggests that the decay kinetics in the region from femtosecond to picosecond is not affected by the defects and/or impurities in the polymer but due to the intrinsic relaxation processes of the excitons, which is not suffers from these defect and/or impurities because of the short observation time.

3.3 Poly(3-dodecylthiophene)

Figure 10 shows the stationary and transient absorption spectra of a P3DT film at 290 K and the pump pulse spectrum. The bleaching due to the depletion of the ground state and the photoinduced absorption below the absorption edge are observed also in P3DT. The absorbance change at 0.0 ps has a large stair at the pump photon energy. The structure is probably due to the induced frequency shift of the probe pulse as observed in the red-phase PDA-4BCMU. A small minimum at 1.80 eV is due to the Raman gain. The corresponding Raman mode is assigned to the stretching vibration of the C=C bond. The bleaching peak at 2.14 eV is due to the 0–1 transition of the same phonon mode. At 0.5 ps the absorbance change around 2 eV becomes positive and the photoinduced absorption has a peak at 1.88 eV. If excitons are assumed to be photoexcited in P3DT by the 1.97 eV pump pulse, this spectral change can be explained by the formation of the relaxed STEs in the same way as PDA-4BCMUs. The time constant of the formation is estimated as 100 ± 50 fs.

P3DT has similar decay kinetics to the red-phase PDA-4BCMU. The decay kinetics has short- und long-lived components. The time constant of the long-lived component is longer than 100 ps. The short-lived component can be fitted to biexponential functions. The sets of the time constants at 290 K are summarized in Table 3. The time constant τ_1 is shorter than 0.5 ps and is expected to correspond the decay of the free excitons. The

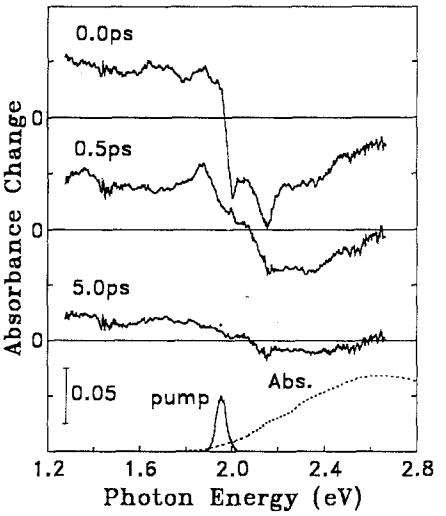

Fig. 10. Transient absorption spectra of a P3DT film at 290 K induced by the 1.97 eV pump pulse. The excitation photon density is 7.5×10^{15} photons/cm^2. The dotted curve is the absorption spectrum

Table 3. Decay time constants of absorbance changes in a P3DT film at 290 K

Probe photon energy [eV]	Time constants [ps]	
	τ_1	τ_2
2.21	0.3 ± 0.1	4.7 ± 1.6
1.88	0.5 ± 0.1	4.7 ± 1.2
1.63	0.3 ± 0.1	7.9 ± 1.8
1.55	0.3 ± 0.1	7.9 ± 2.3

time constant τ_2 corresponds to the decay of the relaxed STEs and is estimated as 4.7 ± 1.2 ps.

If the decay curves are fitted to a power law decay and long-lived component, $\Delta A_1 t^{-\alpha} + \Delta A_L$, the power α at 290 K is obtained as 1.02 ± 0.23 at 2.21 eV, 0.67 ± 0.05 at 1.88 eV, and 0.61 ± 0.06 at 1.63 eV. The power law decay was reported also in other PTs and the value of α was 0.37 in poly(3-hexylthiophene) at 1.17 eV, 0.22 in poly(3-octylthiophene) at 1.17 eV, and 0.9 in polythiophene at 2 eV [29, 30]. The dependence of α on the probe photon energy and the spectral change at the delay time from 0.5 ps to 5 ps are difficult to be explained by a simple recombination model.

Figure 11 shows the time dependence of the absorbance changes at 1.50 eV induced by the pump pulse polarized parallel (//) and perpendicular ($\perp$) to the polymer chains. The short-lived component due to the STEs decreases rapidly and the long-lived component remains much longer than 100 ps. It is clearly see that the long-lived component is induced more efficiency by the perpendicular pump pulse. This means the long-lived component is due to either polarons or bipolarons generated by the interchain photoexcitation. A polaron pair is formed from an electron–hole pair excited by a single photon, while a bipolaron is generated by a collision of two polarons with charge of the same sign. The observed intensity dependence shows that the long-lived component in P3DT increases proportionally to the pump photon density up to 2×10^{16} photons/cm^2. Hence the long-lived component in P3DT is concluded to be due to polarons.

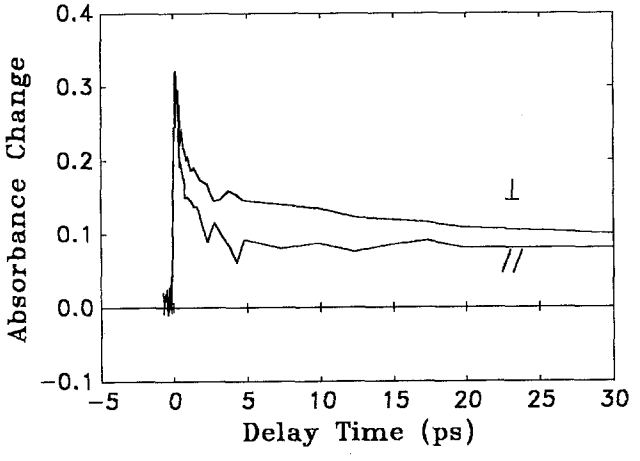

Fig. 11. Time dependence of absorbance changes at 1.50 eV in an oriented P3DT film at 10 K. The polarizations of the pump pulses are parallel (||) and perpendicular ($\perp$) to the polymer chain

4 Relaxation Model of Exciton

All the conjugated polymers observed in this study have similar transient absorption and bleaching spectra and relaxation kinetics to each other. The photoinduced absorbance changes just after excitation have the broad absorption below the absorption edge and the bleaching due to the depletion of the ground state. The broad photoinduced absorption shifts to higher energy with time from 0.0 ps to 0.5 ps. The transient absorbance change has a component which disappear with the time constant of a few picoseconds. The semilogarithmic plots of the absorbance changes, from which the long-lived components due to triplet excitons and/or polarons are subtracted, in several conjugated polymers at 290 K are shown in Fig. 12. The decay curves in blue phase PDAs can be fitted relatively well to single-exponential functions, while the decay in red-phase PDAs and P3DT become slower after the initial fast decay.

The decay kinetics in the blue-phase PDAs have the same time constants within the experimental error. The lifetime is 1.6 ± 0.1 ps in the oriented PDA-4BCMU film, 1.6 ± 0.2 ps in the PDA-3BCMU cast film, and 1.5 ± 0.1 ps in microcrystals of PDA-3BCMU vacuum-deposited on a KCl substrate [47]. The decay kinetics in the cast and oriented films of red-phase PDA-4BCMU have also similar time constants to each other. The time constants at 1.77 eV are 810 ± 60 fs and 10.0 ± 0.6 ps in the cast film and 840 ± 60 fs and 10.9 ± 1.8 ps in the oriented film. The decay kinetics up to several picoseconds in PDAs is independent of the preparation method and the sample quality, but depends on the phase. The ultrafast decay kinetics is concluded to be due to the intrinsic decay processes of the excitons.

The relaxation processes of the excitons in conjugated polymers are explained by the model shown in Fig. 13. One-dimensional systems has no barrier between the potential curves of the free exciton (FE) and the STE. Since the excitons in conjugated polymers are strongly coupled with the C—C stretching modes in the main chain, the geometrical relaxation of STEs is considered to be the change of the bond orders. In PDAs the acetylenic main chain may relax to the butatrienic chain. Both PDAs and PTs correspond to type II by Toyozawa's classification [48]. In type II the crossing point between the STEs and the ground-state potential curves is lower than the bottom of the FE potential curve. The crossing point in blue-phase PDAs (Fig. 13a) is expected to be higher than the point in red-phase PDAs (Fig. 13b) because of the smaller exciton energy in blue-phase PDAs. The relaxation from FE to the bottom of the potential curve of STE and the relaxation from STE to the ground state take place simultaneously. The obtained time constants of the relaxation processes are summarized in Table 4.

Since there is no barrier on the adiabatic potential representing the self-trapping process in one-dimensional systems, the formation of the STE is expected to take place within the coupled phonon cycle [49]. The excitons in conjugated polymers are strongly coupled with the stretching modes of carbon atoms in the main chain. The frequencies of the stretching modes are 1500–2100 cm^{-1}

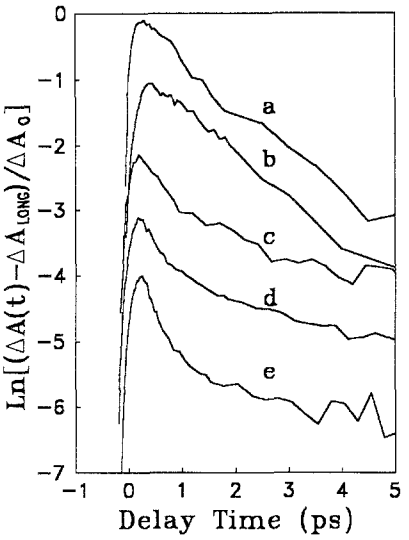

Fig. 12. Time dependence of the absorbance changes at 290 K plotted in a semilogalithmic scale. *(a)* A blue-phase oriented PDA-4BCMU film at 1.88 eV, *(b)* a blue-phase PDA-3BCMU cast film at 1.88 eV, *(c)* a red.phase oriented PDA-4BCMU film at 1.77 eV, *(d)* a red-phase PDA-4BCMU cast film at 1.77 eV, and *(e)* a P3DT film at 1.88 eV. The pump photon energy is 1.97 eV. The long-lived components are subtracted from the observed absorbance changes

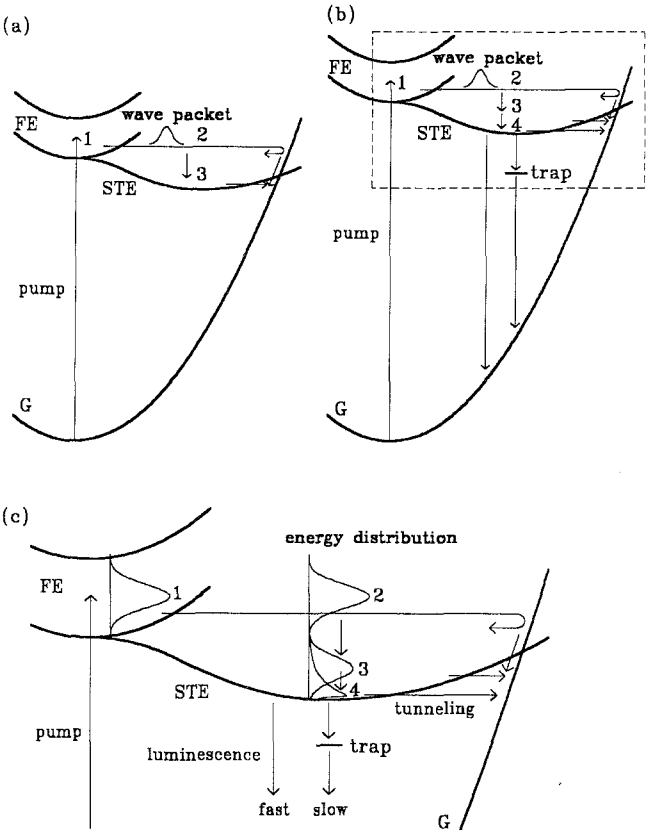

Fig. 13a–c. Models of relaxation kinetics shown in adiabatic potential surfaces of excitons in **a** blue-phase PDAs, **b** red-phase PDAs and PTs, and **c** a magnification of **b**. FE: free exciton, STE: self-trapped exciton, G: ground state, *1* free exciton *2* unrelaxed STE, *3* unthermalized (relaxed) STE, and *4* thermalized STE. Relaxation processes are *1–2* self-trapping, *2–3* phonon emission, and *3–4* thermalization. The time constants of relaxation processes are summarized in Table 3

and correspond to the oscillation periods of 22–16 fs. However, the trapping time constants of excitons are 100–150 fs and are much longer than the phonon periods. It can be explained as follows. The photoexcited FEs are coupled with the C–C stretching modes within the phonon periods of 10–20 fs. However, the STEs have not relaxed to the bottom of the potential curve and the binding energy of the STEs remains as the kinetic energy of the lattice oscillation (unrelaxed STEs).

The unrelaxed STEs emit phonons and relax to the bottom of the potential. The time constant of the phonon emission is determined by the energy redistribution rate from the strongly coupled phonon to the other low-frequency phonon modes The phonon emission process is equivalent to the formation process of the relaxed STEs which was observed as the spectral change with the time constant of 100–150 fs. The time constant of the phonon emission process in P3DT is 100 ± 50 fs and is slightly shorter than in PDAs. It is considered to be due to the rigid ring structures of the main chain and its higher frequency phonon modes. P3MT has even shorter time constant of 70 ± 50 fs [28], because the side group of P3MT is much smaller than P3DT.

The relaxed STEs after the phonon emission process still remain in the unthermalized states. The unthermalized STEs are coupled with phonon modes of low frequency and thermalize. The thermalization process is

Table 4. Time constants of the relaxation processes of exitons at 290 K

Relaxation processes[a]	PDA-4BCMU (blue)	PDA-4BCMU (red)	P3DT
1–2 (self-trapping)[b]	(10–20 fs)	(10–20 fs)	(10–20 fs)
2–3 (phonon emission)	140 ± 40 fs	120 ± 60 fs	100 ± 50 fs
3–4 (thermalization)	–[c]	1.1 ± 0.1 ps	1.0 ± 0.2 ps
2–G (relaxation from unrelaxed STE)	<1.0 ps	0.7 ± 0.1 ps[d]	0.3 ± 0.1 ps[d]
3–G (relaxation from unthermalized STE)	1.6 ± 0.1 ps		
4–G (relaxation from thermalized STE)	–	4.4 ± 0.5 ps	4.7 ± 1.2 ps

[a] 1–4, and G are the states shown in Fig. 13
[b] The time constants of the self-trapping processes could not be time-resolved in this study
[c] The thermalization process could not be detected in the blue-phase PDA
[d] The relaxation to the ground state from the unrelaxed STE and from the unthermalized STE could not be separated

observed as the spectral change with time from 0.5 ps to 5.0 ps. The obtained time constant of the thermalization process is about 1 ps in both red-phase PDAs and P3DT. However, the temperature of the STEs defined from equilibrated vibrational modes after this 1 ps thermalization process may be still higher than the bulk temperature of the whole polymer. Therefore, the cooling down process with time constant of several or a few tens picoseconds is expected to take place after the observed thermalization process. However the spectral change due to the cooling down process of the STEs could not be detected in this study because of limited signal to noise ratio of the spectral data.

The change of the decay rate observed in the red-phase PDA-4BMCU and P3DT can be explained by the thermalization process. The STEs relax to the ground state mainly by tunneling through the barrier between the STEs and ground-state potentials. The time constant of the initial fast decay is shorter than 1 ps. The initial decay is expected to be due to the relaxation to the ground state from both the unrelaxed and unthermalized STEs. The spectral change due to the phonon emission in the red-phase PDAs is not as clear as that in the blue-phase PDAs and the absorbance changes due to the unrelaxed and relaxed STEs have similar spectra. Therefore, the relaxations from the unrelaxed STEs and from the unthermalized STEs could not be distinguished in the red-phase PDA. After the thermalization the STEs come down to the bottom of the potential and the loss rate by the tunneling becomes slower. The decay time constant of about 5 ps is due to the tunneling from the thermalized STE. The thermalization process of the STE is estimated as 1.0 ± 0.1 ps from the spectral change. The wavelength dependence of the decay curve can be explained by the thermalization process. The absorbance change at 2.00 eV in the red-phase PDAs is mainly due to the unthermalized STEs and the thermalized STEs have the absorption peak at 1.6 eV. Therefore, the decay curve at 2.00 eV can be fitted to a single exponential function with the time constant of about 1 ps. The time constant of the absorbance change below 1.8 eV is longer than that of the bleaching, because the unthermalized STEs thermalize with the time constant of 1 ps and the absorption peak due to the thermalized STEs appears at 1.6 eV. The observed data in P3DT can be explained in the same way.

The decay of the relaxed STE in blue-phase PDAs is faster than in red-phase, because the crossing point is lower than the point in red-phase PDAs. The major part of the STEs relax to the ground state before thermalization. The decay rate from the unthermalized (relaxed) STEs to the ground state is not much slower than the decay rate from the unrelaxed STEs. Therefore, the decay curves in the blue-phase PDAs can be fitted to single-exponential functions. The wavelength dependence of the time constant is due to the mixed signals of the STE states. The bleaching signal exhibits both the unrelaxed and unthermalized STEs, while the absorption around 1.8 eV is due to the unthermalized STEs. Therefore, the observed decay time constant of the bleaching is shorter.

The difference between fluorescent and nonfluorescent polymers is the time constant of the tunneling from the unthermalized and thermalized STEs to the ground state. The time constant in the blue-phase is 1.6 ps and is shorter than that in the red-phase PDAs. Therefore the number of the remaining STE in the blue-phase PDA is smaller and the luminescence could not be detected. The fast component of the luminescence in the red-phase PDAs is considered to be due to the free excitons and/or STEs and the slow component is due to the traps in the polymer chains.

The proposed relaxation model predicts that the decay rate of the STE in conjugated polymers depends on the exciton energy. Conjugated polymers with large exciton energy are considered to have excitons with long lifetime and to be more fluorescent. For example poly(*p*-phenylenevinylene) (PPV) which has an absorption peak at 2.5 eV has strong luminescence with a quantum yield of several prescent [50]. Recently, a Langumuir-Blodgett film of PDA-(12,8), which has an exciton peak at 1.88 eV has been studied and the decay time constant of the STE is estimated as 1.3 ± 0.1 ps at 290 K [51]. It is shorter than the that in blue-phase PDAs which have an exciton peak at 1.97 eV. These results are consistent with the proposed model. However, PDA under the hydrostatic pressure has different decay kinetics. When the pressure increases, the absorption edge of red-phase PDA-4BCMU shifts to lower energy but the decay kinetics becomes slower [52]. This pressure effect is probably due to a subsequent three-dimensional distortion of the polymer chain. The decay kinetics under the pressure may be different from that in the one-dimensional system.

5 Conclusion

The ultrafast optical responses in blue- and red-phase PDA-4BCMU and P3DT films have been investigated. The bleaching due to the depletion of the ground state and the photoinduced absorption below the absorption edge have been observed in both PDA-4BCMUs and P3DT by the femtosecond absorption spectroscopy. When the pump and the probe pulses overlap in time at the sample, spectral changes due to several nonlinear optical processes, i.e., hole burning, Raman gain, inverse Raman scattering, and induced-frequency shift, have been observed. The luminescence in the red-phase PDAs has fast and slow component. The fast component is probably due to the free excitons and/or STEs and the slow components is due to the traps in the polymer chains.

The relaxation kinetics of the photoexcitations in the conjugated polymers is explained in terms of the STEs using the same model. The difference between the decay kinetics in blue-phase and red-phase PDAs is explained in terms of the exciton energy. The relaxation from photoexcited free excitons to STEs has been observed in both PDA-4BCMU and P3DT. The relaxation processes can be classified as the self-trapping process, the phonon emission process, and the thermalization process. The relaxation from the STEs to the ground state is mainly due to the tunneling in configuration space. The decay

kinetics of the STEs in the blue-phase PDA-4BCMU can be fitted to the single-exponential function with time constant of 1.6 ± 0.1 ps at 290 K. The decay kinetics in the red-phase PDA-4BCMU and P3DT cannot be fitted to single-exponential functions but can be fitted to biexponential functions with time constants of 0.6 ± 0.1 and 4.4 ± 0.4 ps in the red-phase PDA-4BCMU and 0.3 ± 0.1 and 4.7 ± 1.2 ps in P3DT. The two decay time constants in the biexponential functions correspond to the tunneling from the unrelaxed and unthermalized STEs and from the thermalized STEs, respectively.

Acknowledgements. We thank H. Uchiki, T. Gima, U. Stamm, and M. Taiji for assistance in the construction of the femtosecond system and K. Yoshino for providing us with P3DT films. Valuable discussions with Profs. Y. Toyozawa, E. Hanamura, and H. Sumi are also gratefully acknowledged. This research was partly supported by the Kurata Research grant from the Kurata Foundation and a grant from the Itoh Science Foundation to M. Y. and T. K. and a grant from the Toray Science Foundation to T. K.

References

1. See, e.g., T. Kobayashi (ed.): *Nonlinear Optics of Organics and Semiconductors*, Springer Proceeding Physics, Vol. 36 (Springer, Berlin, Heidelberg 1989)
2. W.-S. Fann, S. Benson, J.M.J. Madey, S. Etemad, G.L. Baker, F. Kajzar: Phys. Rev. Lett. **62**, 1492 (1989)
3. A.J. Heeger, S. Kivelson, J.R. Scrieffer, W.-P. Su: Rev. Modern Phys. **60**, 781 (1988)
4. M. Sinclair, D. Moses, K. Akagi, A.J. Heeger: Phys. Rev. B **38**, 10724 (1988)
5. C.V. Shank, R. Yen, R.L. Fork, J. Orenstein, G.L. Baker: Phys. Rev. Lett. **49**, 1660 (1982)
6. L. Rothberg, T.M. Jedju, S. Etemad, G.L. Baker: IEEE J. QE-**24**, 311 (1988)
7. M. Yoshizawa, T. Kobayashi, K. Akagi, H. Shirakawa: Phys. Rev. B **37**, 10301 (1988)
8. P.D. Townsend, R.L. Friend: Phys. Rev. B **40**, 3112 (1989)
9. See, e.g., D. Bloor, R.R. Chance (eds.): Polydiacetylenes (Martinus Nijhoff, Dordrecht 1985)
10. S. Koshihara, Y. Tokura, K. Takeda, T. Koda, A. Kobayashi: J. Chem. Phys. **92**, 7581 (1990)
11. R.R. Chance, G. Patel, J.D. Witt: J. Chem. Phys. **71**, 206 (1979)
12. K.S. Wong, W. Hayes, T. Hattori, R.A. Taylor, J.F. Ryan, K. Kaneto, K. Yoshino, D. Bloor: J. Phys. C **18**, L 843 (1985)
13. A. Kobayashi, H. Kobayashi, Y. Tokura, T. Kanetake, T. Koda: J. Chem. Phys. **87**, 4962 (1987)
14. T. Hattori, T. Kobayashi: Chem. Phys. Lett. **133**, 230 (1987)
15. G.M. Carter, J.V. Hryniewicz, M.K. Thakur, Y.J. Chen, S.E. Meyler: Appl. Phys. Lett. **49**, 998 (1986)
16. C.C. Hsu, Y. Kawabe, Z.Z. Ho, N. Peyghambarian, J.N. Polky, W. Krug, E. Miao: J. Appl. Phys. **67**, 7199 (1990)
17. T. Hasegawa, K. Ishikawa, T. Kanetake, T. Koda, K. Takeda, H. Kobayashi, K. Kubodera: Chem. Phys. Lett. **171**, 239 (1990)
18. J. Swiatkiewicz, X. Mi, P. Chopra, P.N. Prasad: J. Chem. Phys. **87**, 1882 (1987)
19. G.J. Blanchard, J.P. Heritage: J. Chem. Phys. **93**, 4377 (1990)
20. P.P. Ho, N.L. Yang, T. Jimbo, Q.Z. Wang, R.R. Alfano: J. Opt. Soc. Am. B **4**, 1025 (1987)
21. F. Charra, J.M. Nunzi: *Organic Molecules for Nonlinear Optics and Photonics*, ed. by J. Messier et al. (Kluwer, Dordrecht 1991) p. 359
22. T. Kobayashi, M. Yoshizawa, U. Stamm, M. Taiji, M. Hasegawa: J. Opt. Soc. Am. B **7**, 1558 (1990)
23. F. Kajzar, L. Rothberg, S. Etemad, P.A. Chollet, D. Grec, A. Boudet, T. Jedju: Opt. Commun. **66**, 55 (1988)
24. S. Koshihara, T. Kobayashi, H. Uchiki, T. Kotaka, H. Ohnuma: Chem. Phys. Lett. **114**, 446 (1985)
25. M. Yoshizawa, M. Taiji, T. Kobayashi: IEEE J. QE-**25**, 2532 (1989)
26. B.I. Greene, J. Orenstein, R.R. Millard, L.R. Williams: Chem. Phys. Lett. **139**, 381 (1987)
27. J.M. Huxley, P. Mataloni, R.W. Schoenlein, J.G. Fujimoto, E.P. Ippen, G.M. Carter: Appl. Phys. Lett. **56**, 1600 (1990)
28. U. Stamm, M. Taiji, M. Yoshizawa, T. Kobayashi, K. Yoshino: Mol. Cryst. Liq. Cryst. A **182**, 147 (1990)
29. D. McBranch, A. Heys, M. Sinclair, D. Moses, A.J. Heeger: Phys. Rev. B **42**, 3011 (1990)
30. Z. Vardeny, H.T. Grahn, A.J. Heeger, F. Wudl: Synth. Metals **28**, C 299 (1989)
31. I.D.W. Samuel, K.E. Meyer, R.H. Friend, J. Rühe, G. Wegner: Synth. Metals **41**, 1399 (1991)
32. Z. Vardeny, E. Ehrenfreund, O. Brafman, M. Nowak, H. Schaffer, A.J. Heeger, F. Wudl: Phys. Rev. Lett. **56**, 671 (1986)
33. N. Colerani, M. Nowak, D. Spiegel, S. Hotta, A.J. Heeger: Phys. Rev. B **36**, 7964 (1987)
34. K. Kaneto, S. Hayashi, K. Yoshino: Jpn. J. Phys. Soc. **57**, 1119 (1988)
35. K. Kaneto, F. Uesugi, K. Yoshino: Solid State Commun. **65**, 783 (1987)
36. T. Kanetake, K. Ishikawa, T. Koda, Y. Tokura, K. Takeda: Appl. Phys. Lett. **51**, 1957 (1987)
37. M. Yoshizawa, T. Kobayashi, H. Fujimoto, J. Tanaka: Phys. Rev. B **37**, 8988 (1988)
38. D. Bloor, S.D.D.V. Rughooputh, D. Phillips, W. Hayes, K.S. Wong: *Electronic Properties of Polymers and Related Compounds*, ed. by H. Kuzmany, M. Mehring, S. Roth, Springer Series Solid-State Sc., Vol. 63 (Springer, Berlin, Heidelberg 1985) p. 253
39. J. Orenstein, S. Etemad, G.L. Baker: J. Phys. C **17**, L 297 (1984)
40. L. Robins, J. Orenstein, R. Superfine: Phys. Rev. Lett. **56**, 1850 (1986)
41. K. Ichimura, M. Yoshizawa, H. Matsuda, S. Okada, M. Osugi, S. Hourai, H. Nakanishi, T. Kobayashi: Submitted
42. H. Sumi, M. Georgiev, A. Humi: Rev. Solid State Sci. **4**, 209 (1990)
43. J.P. Sokoloff, M. Joffre, B. Fluegel, F. Hulli, M. Lindberg, S.W. Koch, A. Migus, A. Antonetti, N. Peyghambarian: Phys. Rev. B **38**, 7615 (1988)
44. C.H. Brito Cruz, J.P. Gordon, P.C. Becker, R.L. Fork, C.V. Shank: IEEE J. QE-**24**, 261 (1988)
45. P.L. Baldeck, R.R. Alfano, G.P. Agrawal: Appl. Phys. Lett. **52**, 1939 (1988)
46. E. Tokunaga, A. Terasaki, K. Tsunetomo, Y. Osaka, T. Kobayashi: Submitted
47. M. Yoshizawa, H. Hattori, T. Kobayashi: Submitted
48. Y. Toyozawa: Jpn. J. Phys. Soc. **58**, 2626 (1989)
49. K. Nasu: J. Lumin. **38**, 90 (1987)
50. R.H. Friend, D.D.C. Bradley, P.D. Townsend: J. Phys. D **20**, 1367 (1987)
51. M. Yoshizawa, K. Nishiyama, M.Fujihira, T. Kobayashi: Submitted
52. B.C. Hess, G.S. Kanner, Z.V. Vardeny, G.L. Baker: Phys. Rev. Lett. **66**, 2364 (1991)